Diverse cataclysmic floods from Pleistocene glacial Lake Missoula

Chapter · October 2020

DOI: 10.1130/2021.2548(17)

5 authors, including:

Roger Denlinger
United States Geological Survey

David L. George
United States Geological Survey

The Geological Society of America
Special Paper 548

Diverse cataclysmic floods from Pleistocene glacial Lake Missoula

Roger P. Denlinger
David L. George
Cascades Volcano Observatory, U.S. Geological Survey,
1300 SE Cardinal Court, Building 10, Vancouver, Washington 98683, USA

Charles M. Cannon
Jim E. O'Connor
U.S. Geological Survey, 2130 SW 5th Avenue, Portland, Oregon 97201, USA

Richard B. Waitt
Cascades Volcano Observatory, U.S. Geological Survey,
1300 SE Cardinal Court, Building 10, Vancouver, Washington 98683, USA

ABSTRACT

In late Wisconsin time, the Purcell Trench lobe of the Cordilleran ice sheet dammed the Clark Fork of the Columbia River in western Montana, creating glacial Lake Missoula. During part of this epoch, the Okanogan lobe also dammed the Columbia River downstream, creating glacial Lake Columbia in northeast Washington. Repeated failure of the Purcell Trench ice dam released glacial Lake Missoula, causing dozens of catastrophic floods in eastern Washington that can be distinguished by the geologic record they left behind. These floods removed tens of meters of pale loess from dark basalt substrate, forming scars along flowpaths visible from space.

Different positions of the Okanogan lobe are required for modeled Missoula floods to inundate the diverse channels that show field evidence for flooding, as shown by accurate dam-break flood modeling using a roughly 185 m digital terrain model of existing topography (with control points dynamically varied using automatic mesh refinement). The maximum extent of the Okanogan lobe, which blocked inundation of the upper Grand Coulee and the Columbia River valley, is required to flood all channels in the Telford scablands and to produce highest flood stages in Pasco Basin. Alternatively, the Columbia River valley must have been open and the upper Grand Coulee blocked to nearly match evidence for high water on Pangborn bar near Wenatchee, Washington, and to flood Quincy Basin from the west. Finally, if the Columbia River valley and upper Grand Coulee were both open, Quincy Basin would have flooded from the northeast.

In all these scenarios, the discrepancy between modeled flood stages and field evidence for maximum flood stages increases in all channels downstream, from Spokane to Umatilla Basin. The pattern of discrepancies indicates that bulking of floods by loess increased flow volume across the scablands, but this alone does not explain low

Denlinger, R.P., George, D.L., Cannon, C.M., O'Connor, J.E., and Waitt, R.B., 2021, Diverse cataclysmic floods from Pleistocene glacial Lake Missoula, *in* Waitt, R.B., Thackray, G.D., and Gillespie, A.R., eds., Untangling the Quaternary Period—A Legacy of Stephen C. Porter: Geological Society of America Special Paper 548, https://doi.org/10.1130/2021.2548(17).

modeled flow stages along the Columbia River valley near Wenatchee. This latter discrepancy between modeled flood stages and field data requires either additional bulking of flow by sediment along the Columbia reach downstream of glacial Lake Columbia, or coincident dam failures of glacial Lake Columbia and glacial Lake Missoula.

INTRODUCTION

In late Wisconsin time, the Cordilleran ice sheet advanced into northeastern Washington and northern Idaho in the western United States (Fig. 1) and at times simultaneously dammed the flow of the Columbia River in multiple places. Subsequent ice-dam ruptures then produced catastrophic flooding of eastern Washington. The evidence for massive flooding was recognized first by Bretz (1923, 1925, 1928a) and then greatly extended later with field studies by Baker (1973), Waitt (1980, 1984, 1985), Atwater (1986), Benito and O'Connor (2003), and O'Connor and Baker (1992). The Purcell Trench lobe of the ice sheet dammed the Clark Fork to form the large glacial Lake Missoula, which gives these floods their name. At times, the Okanogan ice lobe also blocked the Columbia River valley near the entrance of upper Grand Coulee to form a much smaller glacial Lake Columbia (Atwater, 1986, 1987).

Stratigraphic evidence in back-flooded valleys shows that there were dozens of floods (Waitt, 1980, 1985, 1994; Atwater, 1986), and the relative timing of blockages by these two ice lobes caused distinctive patterns of flooding. Whether or not the Okanogan lobe blocked the Columbia River at the times when the Purcell lobe ice dam ruptured altered both the timing and distribution of these glacial outburst floods. These floods had an enormous impact on the landscape, carving and modifying large-scale landforms and leaving deposits that dominate much of the geomorphology of eastern Washington. This geomorphic evidence provides a means to distinguish between initial conditions for these floods, and to determine whether the Okanogan blockage existed or whether upper Grand Coulee was open during each Missoula flood.

The effects of these catastrophic flows are impressive. They include large-scale dunes (Fig. 2A), which are much larger versions of the dunes formed by ordinary river flows (Bretz, 1928a), widespread erosion of loess and its basalt substrate (Figs. 2B and 2C) to form scablands (Bretz, 1928b), and repetitive layers of fine sediment deposition in slack-water areas such as Burlingame Canyon (Fig. 2D) that record the passage of dozens of floods (Waitt, 1980, 1984, 1985, 1994; Atwater, 1984, 1986, 1987; Benito and O'Connor, 2003; Hanson et al., 2012). Erosion of 30–40 m of loess by flooding of the Telford and Cheney-Palouse scabland tracts (Figs. 1 and 2B) left many teardrop-shaped plateaus as remnants (Fig. 2C).

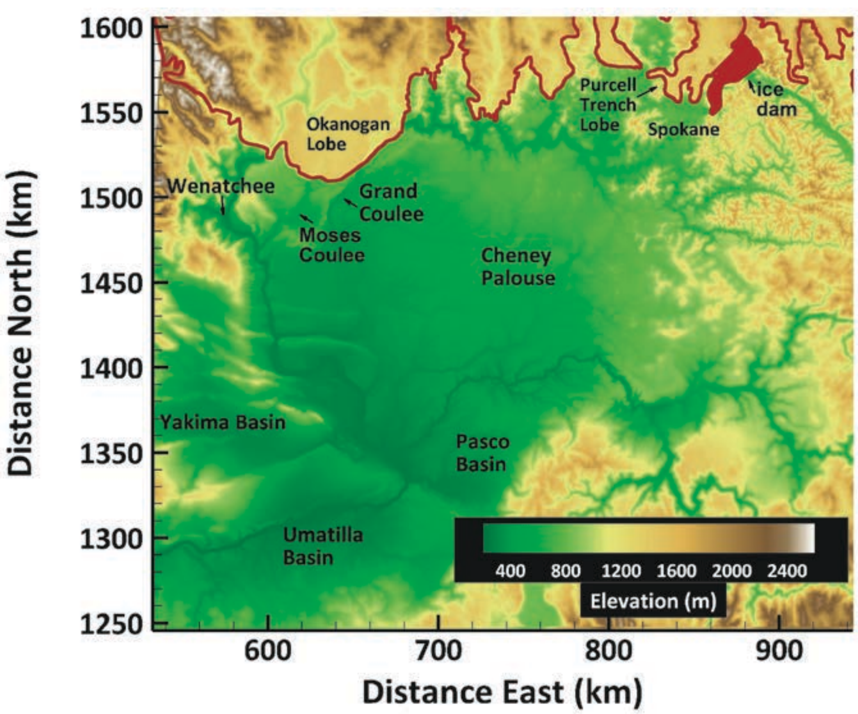

Figure 1. Portion of the digital terrain in eastern Washington used to route the flows for the first 72 h of the simulation, showing the Columbia River valley, the locations of the Okanogan and Purcell Trench lobes, and the scablands and the large basins that hold the water dammed by the Columbia River Gorge (off the map to the west). Grid and terrain map produced with an Albers projection with a NAD 1983 reference. The margin of the continental ice sheet encroaching from the north is shown as a red line, with the portion of the Purcell Trench lobe that formed the ice dam for glacial Lake Missoula shown in the solid red polygon. The solid red polygon is all glacial ice that is initially tunneled and then removed once the dam fails. The Columbia and Snake River channels are green or dark green on lighter or different color backgrounds, with the Columbia River valley blocked by the Okanogan lobe north of Grand Coulee to form glacial Lake Columbia. South from this lobe blockage, the Columbia channel heads into Quincy and Pasco Basins. Post dam-break flooding of this large (green) area takes about 3 d, after which time floodwaters are ponded in Pasco and Umatilla Basins. Floodwaters drain through the Columbia River Gorge (just west of Umatilla Basin) much more slowly than these basins fill, and once filled, it then takes many weeks to drain all floodwaters through the Columbia River Gorge.

Scabland scars from these floods (shown by remarkable Landsat Multispectral Scanner System (MSS) satellite images (www.mines.edu/academic/geology/faculty/klee/missoula.doc) in Figure 3, mark locations where multiple floods eroded light-colored windblown loess from a dark underlying basalt substrate. The Landsat photos, showing scars over thousands of square kilometers, indicate large scale, massive transport of fine sediment by these floods. Past depth-averaged flow modeling of a single large flood supports this field evidence, as the distribution of highly erosive stream power matches the intricate pattern of erosion made by these floods (Denlinger and O'Connell, 2010).

Comprehensively, detailed flow models for these flows are constrained by a wide variety of field data, providing insights into the processes and timing of inundation. These diverse field data include the locations of flood scars, locations of ice-rafted erratics, evidence for inundation of low points in ridges (Table 1), and evidence for lake levels and residence times for both glacial Lake Missoula and glacial Lake Columbia (Atwater, 1987). We now have more evidence (Table 1) than was published in 2009 when Denlinger and O'Connell (2010) modeled a single flood, more accurate topography, and more evidence distinguishing different floods. In addition, recent improvements in numerical models for floods (George, 2008, 2011) more accurately calculate

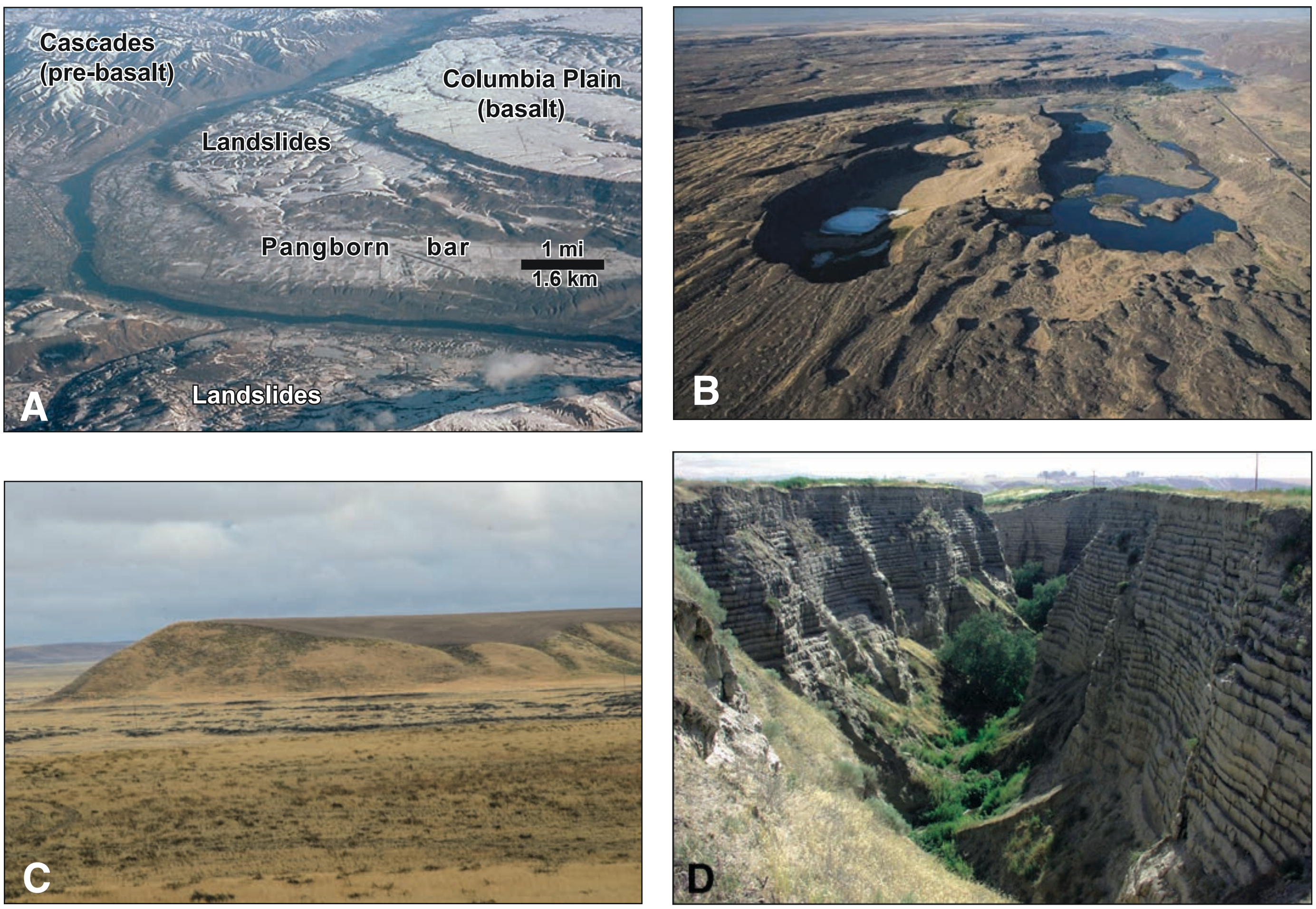

Figure 2. (A) Oblique aerial photograph of Pangborn bar, looking north. Snow highlights giant current dunes with a wavelength of about 130 m across the top of the bar. Each dune has a steep south-facing lee side, showing that these dunes were built by one or more floods flowing north to south downvalley. Platted city of Wenatchee is west of Columbia River on the left margin of the photo. Photograph was taken February 1972 by R.B. Waitt. (B) Removal of loess and erosion of basalt by floods flowing from north (bottom of photo) to south (top of photo) created this scabland topography at Dry Falls, Washington. The lake on the right is ~0.6 km across (left to right). Photo by Bruce Bjornstad; used with permission. (C) Erosion of loess in the Cheney-Palouse scabland left large plateaus of loess 30 to 50 m high and hundreds of meters long and wide scattered throughout the scablands. Photo by Richard Waitt, taken on 16 September 2019, north of Marengo, Washington, in the southern Cheney-Palouse scabland. View is to the SE, and the height of the scarp is 50 m. An aerial photo of a large loess island in the Cheney Palouse tract, illustrating a teardrop shape, can be found at https://news.nationalgeographic.com/2017/03/channeled-scablands. (D) Eroded material from floods (parts B and C) was carried as suspended load into slack-water areas such as Burlingame Canyon, shown here. Each layer was deposited from a different flood, and the average thickness on the right-hand side of the photo is about 20 cm. Photo by Bruce Bjornstad; used with permission.

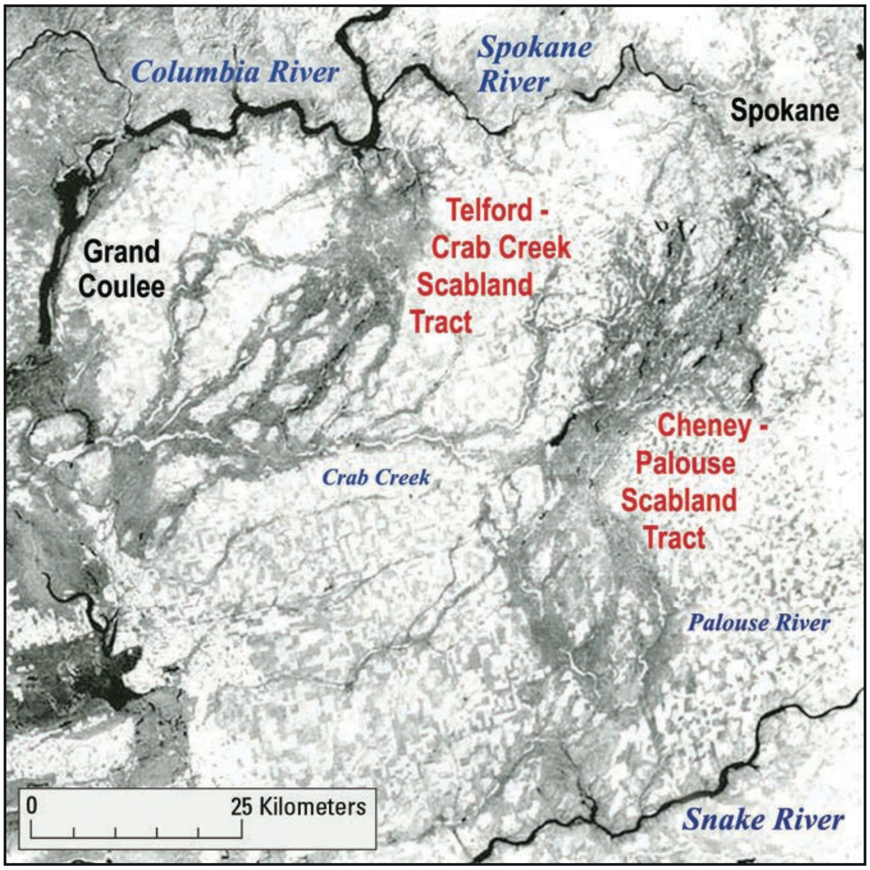

Figure 3. Landsat image of the scars left by massive, late Wisconsin floods in eastern Washington, as floods washed away light-colored loess and scoured the black basalt. The contrast between loess and basalt leaves a stark image of flood passage, revealed by the light- to dark-gray drainage pattern on the light background; used with permission from Keenan Lee.

inundation margins, increasing the resolution needed for comparison with field data by an order of magnitude while simultaneously decreasing computation time.

Other quantitative numerical studies of large-scale flood inundation have been done since Denlinger and O'Connell (2010) modeled large-scale Missoula floods. Among them, those by Abril-Hernández et al. (2018), Bohorquez et al. (2016), and Carling et al. (2010) show that given appropriate initial conditions and boundary conditions, new flood-routing technology can compare different topographic scenarios with field data at local field scales, thereby increasing our understanding of the timing and distribution of multiple floods. We show in this paper that such use of more sophisticated routing programs, increased landscape resolution, and greater knowledge of the flood record can be used effectively to determine the significance of disparate records left by different floods.

Since flood processes are complex and topography in eastern Washington is rugged, sophisticated and detailed numerical models for flow over 3D topography are necessary to simulate the mechanics and patterns of inundation of these large floods. Field evidence in eastern Washington indicates passage of these floodwaters in numerous channels distributed over 60,000 km^2 and over 600 m in elevation. The complexity of these flows cannot be understood with one-dimensional flow models. One-dimensional models, while providing rough estimates when restricted to narrow, approximately linear reaches such as the Columbia River Gorge (Benito and O'Connor, 2003), do not model flow simultaneously diverging into multiple channels (Fig. 3), and they misrepresent a single channel if it has complex topography (Denlinger et al., 2001). The nature and intricacy of distributed overland flow during this repeated, large-scale, late Pleistocene flooding of eastern Washington require, at a minimum, solution of depth-averaged Navier-Stokes flow equations (i.e., LeVeque, 2002) on an accurate digital model of three-dimensional terrain to produce physically meaningful results.

Our application of such a depth-averaged flow model to simulate Lake Missoula floods assumed an instantaneous dam break of the largest glacial Lake Missoula for each scenario. However, each scenario produced different flow paths, and for each, we compared model stage to field evidence for maximum stage and used the timing and magnitude of inundation to understand the differences in flooding. Locations where erosion and deposition were expected to occur were found from model velocities and flow depths. Using this technology, Denlinger and O'Connell (2010) obtained meaningful results using initial conditions and a topography similar to scenario 1b in this study. They found that both inundation and locations of scour matched areas of inundation and scour observed in the field, and showed that multiple channels often drained simultaneously. For example, the Cheney Palouse tract flooded early when flood discharge was high

TABLE 1. DESCRIPTION OF CONTROL POINTS FOR GLACIAL LAKE MISSOULA FLOODS

General location	Feature	Latitude (°N)	Longitude (°W)	Source	Elevation (ft)	Elevation (m)	Elevation source	*x*_albers (m)	*y*_albers (m)	*z*_dtm (m)
Fifteenmile Creek	Erratics	45.6159	120.9491	O'Connor 04-26-2016-10	1120	341	USGS quad, 40 ft contour interval	526043	1283854	341
Fulton Ridge east of Fairbanks Gap	Divide not crossed	45.6359	120.9918	O'Connor interpretation	1200	366	USGS quad, 40 ft contour interval	522746	1286108	360
The Nook at John Day River	Divide crossing	45.6985	120.5281	Benito and O'Connor (2003)	1020	311	USGS quad, 20 ft contour interval	558907	1292731	311
The Nook at John Day River	Divide not crossed	45.6866	120.5008	Benito and O'Connor (2003)	1140	347	USGS quad, 20 ft contour interval	561026	1291392	339
Wallula Gap	Divide crossing	46.0525	118.9910	Bretz (1969); O'Connor and Baker (1992)	1140	347	USGS quad, 20 ft contour interval	678009	1332470	351
Wallula Gap	Unflooded loess; top of loess scarp	46.0519	118.9940	O'Connor interpretation	1223	373	Surveyed section corner	677783	1332404	371
Wallula Gap	Base of loess scarp, near boulder bar	46.0399	118.9038	O'Connor interpretation	1180	360	USGS quad, 20 ft contour interval	684770	1331156	368
Wallula Gap	Top of loess scarp	46.0389	118.9037	O'Connor and Baker (1992)	1240	378	USGS quad, 20 ft contour interval	684784	1331044	373
Wallula Gap	Divide not crossed	46.0336	118.9179	O'Connor interpretation	1220	372	USGS quad, 20 ft contour interval	683694	1330441	367
Sentinel Gap	Divide not crossed	46.8109	119.9475	O'Connor interpretation	1560	475	USGS quad, 20 ft contour interval	604002	1416363	468
Babcock Bench	Stripped basalt	47.1663	119.9780	O'Connor 08-03-2017-01	1370	418	USGS quad, 20 ft contour interval	601667	1455889	415
Lynch Coulee divide crossing	Divide crossing	47.2119	119.9674	O'Connor interpretation	1420	433	USGS quad, 20 ft contour interval	602466	1460960	431
Ginkgo State Park	Erratic	46.9448	120.0263	Balbas (2017, personal commun.)		365	USGS quad, 20 ft contour interval	597999	1431248	366
Wenatchee area, Burch Mountain Road	Erratic	47.4954	120.3312	O'Connor 09-14-2015-09	1550	472	USGS quad, 20 ft contour interval	575051	1492553	467
Wenatchee area, Burch Mountain Road	Erratic	47.4955	120.3310	O'Connor 09-06-2017-01	1560	475	USGS quad, 20 ft contour interval	575068	1492563	467
Wenatchee area (Long site #10)	Erratic	47.4224	120.2027	Waitt et al., 2019 Table 1	1623	495	USGS quad, 20 ft contour interval	584745	1484475	503
Wenatchee area (Long site #11)	Erratic	47.4361	120.2432	Waitt et al., 2019 Table 1	1561	476	USGS quad, 20 ft contour interval	572117	1485888	379
Wenatchee area (Long site #12)	Erratic	47.4435	120.2601	Waitt et al., 2019 Table 1	1584	483	USGS quad, 20 ft contour interval	580392	1486712	476
Grand Coulee	Divide crossing	47.5821	119.2575	Baker (1973) High-water mark 2	1810	552	USGS quad, 10 ft contour interval	655839	1502392	552
Grand Coulee	Erratic	47.5095	119.4741	Baker (1973) High-water mark 3	1790	546	USGS quad, 10 ft contour interval	639603	1494189	538
Grand Coulee	Divide not crossed	47.476	119.3021	Baker (1973) High-water mark 5	1830	558	USGS quad, 10 ft contour interval	652587	1490562	554
Grand Coulee	Divide crossing	47.4734	119.2804	Baker (1973) High-water mark 5	1720	524	USGS quad, 10 ft contour interval	654225	1490287	521
Grand Coulee	Divide not crossed	47.4669	119.2056	Baker (1973) High-water mark 8	1740	530	USGS quad, 20 ft contour interval	659868	1489618	527
Grand Coulee	Divide crossing	47.4689	119.1994	Baker (1973) High-water mark 8	1700	518	USGS quad, 20 ft contour interval	660333	1489845	516

(*Continued*)

TABLE 1. DESCRIPTION OF CONTROL POINTS FOR GLACIAL LAKE MISSOULA FLOODS (*Continued*)

General location	Feature	Latitude (°N)	Longitude (°W)	Source	Elevation (ft)	Elevation (m)	Elevation source	*x*_albers (m)	*y*_albers (m)	*z*_dtm (m)
Grand Coulee	Divide crossing	47.4247	119.4526	Baker (1973) High-water mark 9	1460	445	USGS quad, 20 ft contour interval	641286	1484769	444
Grand Coulee	Divide not crossed	47.4162	119.4426	Baker (1973) High-water mark 10	1520	463	USGS quad, 20 ft contour interval	642047	1483829	457
Quincy Basin via Grand Coulee	Scabland	47.2529	119.5461	Baker (1973) High-water mark 12	1340	408	USGS quad, 10 ft contour interval	634342	1465616	404
Quincy Basin	Divide crossing	47.0493	119.9704	Baker (1973) High-water mark 12	1340	408	USGS quad, 10 ft contour interval	602249	1442872	408
Quincy Basin; Frenchman Coulee	Erratic	46.9442	119.5408	Baker (1973) High-water mark 15	1360	415	USGS quad, 10 ft contour interval	634939	1431280	412
Quincy Basin, Lind Coulee	Erratic	46.9506	119.0373	Baker (1973) High-water mark 16	1350	411	USGS quad, 10 ft contour interval	673239	1432331	410
Quincy Basin, Lind Coulee	Erratic	46.9535	119.3043	Baker (1973) High-water mark 17	1340	408	USGS quad, 10 ft contour interval	652924	1432444	406
Quincy Basin; Frenchman Coulee	Divide not crossed	46.9447	119.5681	Baker (1973) High-water mark 18	1379	420	Checked elevation on USGS quad, 10 ft contour interval	632862	1431324	424
Othello Basin; Crab Creek	Erratic	46.9346	119.5687	Baker (1973) High-water mark 19	1180	360	USGS quad, 10 ft contour interval	632822	1430201	360
Pasco Basin; Saddle Mountains	Divide not crossed	46.7443	119.2192	Baker (1973) High-water mark 20	1210	369	USGS quad, 10 ft contour interval	659624	1409232	366
Pasco Basin; Saddle Mountains	Divide crossing	46.7315	119.2049	Baker (1973) High-water mark 21	1155	352	Checked elevation on USGS quad, 10 ft contour interval	660730	1407819	349
Washtucna Coulee/Snake divide	Divide crossing	46.7021	118.3457	Baker (1973) High-water mark 23		435	USGS quad, 5 m contour interval	726415	1405549	440
Washtucna Coulee/Snake divide	Divide crossing	46.7028	118.3565	Near (or perhaps is) Baker highwater mark 23		410	USGS quad, 5 m contour interval	725588	1405610	413
Washtucna Coulee/Snake divide	Divide not crossed	46.7015	118.3429	Baker (1973) High-water mark 24		450	USGS quad, 5 m contour interval	726630	1405486	444
Washtucna Coulee/Snake divide	Divide crossing	46.7245	118.3105	Baker (1973) High-water mark 25		425	USGS quad, 5 m contour interval	729052	1408096	436
Washtucna Coulee/Snake divide	Divide not crossed	46.6776	118.3474	Baker (1973) High-water mark 26	1360	420	USGS quad, 5 m contour interval	726341	1402821	420
Washtucna Coulee/Snake divide east of Palouse R.	Divide crossing	46.729	118.0395	Baker (1973) High-water mark 28	1660	505	USGS quad, 5 m contour interval	749736	1409066	512
Washtucna Coulee/Snake divide east of Palouse R.	Divide not crossed	46.7353	118.0794	O'Connor interpretation	1670	510	USGS quad, 5 m contour interval	746673	1409693	494
Washtucna Coulee/Snake divide east of Palouse R.	Divide crossing	46.7357	118.0735	O'Connor interpretation	1510	460	USGS quad, 5 m contour interval	747122	1409749	461
Evergreen-Babcock Ridge	Divide not crossed	47.0956	119.9602	Waitt interpretation		419	USGS quad			
Evergreen-Babcock Ridge	Divide not crossed	47.2118	119.9687	Waitt interpretation		431	USGS quad			
Saddle near Camden Gap	Divide not crossed	48.0808	117.1970	Waitt et al. (2019)		880	USGS quad			
Camden Gap	Divide crossed	48.0813	117.2239	Waitt et al. (2019)		795	USGS quad			

Note: Entries shaded in gray are nonexceedance bounds on flood stage. Coordinates are in World Geodetic System 1984 (WGS84). USGS—U.S. Geological Survey; R.—River; *x*/*y*_albers—Albers (equal-area) projection, North American Datum of 1983; z_dtm—digital terrain model on which simulations were run. 1 ft = 0.3048 m.

enough near Spokane, Washington, to top a saddle giving the flow access into Snake valley to the south, even as flooding continued westward along the main channel. Farther downstream, they were the first to show that the Columbia River Gorge (the canyon of the Columbia River through the Cascade Range) was the tightest bottleneck for drainage to the sea; it held up flow for weeks, whereas Wallula Gap (the narrow channel between Pasco and Umatilla Basins) only delayed flow for a few hours as Umatilla Basin filled. Within three days after each dam break, the Columbia River Gorge had dammed almost all floodwaters draining from eastern Washington, storing this water in Umatilla, Pasco, and Yakima Basins. As in our study here, complete drainage to the sea then took many weeks (Denlinger and O'Connell, 2010). All these results debunk the paradigm that Wallula Gap was a significant impediment to flow (Bretz, 1925; O'Connor and Baker, 1992). Despite this new insight of flood drainage, many questions remain unanswered about the field evidence that indicates passage of these floods.

Field data now establish that there were mutually exclusive pathways for multiple late Wisconsin floods, proving that different initial conditions need to be considered in studies of these floods. There cannot have been both an open Columbia River valley and a glacial Lake Columbia at the time each dam break occurred, yet field evidence supports both flooding of an open Columbia River valley during some floods and blockage of that channel during others (Atwater, 1986, 1987). The end-member scenario of an open Columbia River valley and open upper Grand Coulee and the other end-member scenario of a closed channel and closed upper Grand Coulee bracket four other scenarios that are variants of these two initial conditions. These six scenarios help to explain what we see in the field, as each scenario results in substantial differences in the catastrophic flooding of eastern Washington. These differences are the subject of this report.

FIELD EVIDENCE

Field evidence for maximum flood stages consists of flow-crossed divides, eroded channels, erosional trim lines, and the upper extent of diverse flood deposits (including ice-rafted erratics; Bretz, 1923, 1928b, 1929; Baker, 1973; O'Connor and Baker, 1992; Benito and O'Connor, 2003; Waitt et al., 2009, 2019; Waitt, 2016). We summarize some of this in Table 1, and locations are shown in Figure 4. Such features document stages met or exceeded by at least one Missoula flood. Upper flood limits were determined partly by elevations that field observations showed were *not* flooded. For instance, divides covered by uneroded loess gave maximum-limiting heights of peak-flood level. Flat-bottomed channels bounded by sharp, steep margins gave minimum heights of flood in such loess-covered uplands.

The strongest limits on stage came from a combination of a definitive limit not exceeded (i.e., a divide not crossed) not far from similar evidence of flooding such as a high divide-saddle crossed or high ice-rafted erratic. This juxtaposition brackets the maximum flood level at those locations. A weaker stage constraint is a single deposit such as a gravel bar or a graded bed, or an ice-rafted erratic—a minimum bound on stage that could

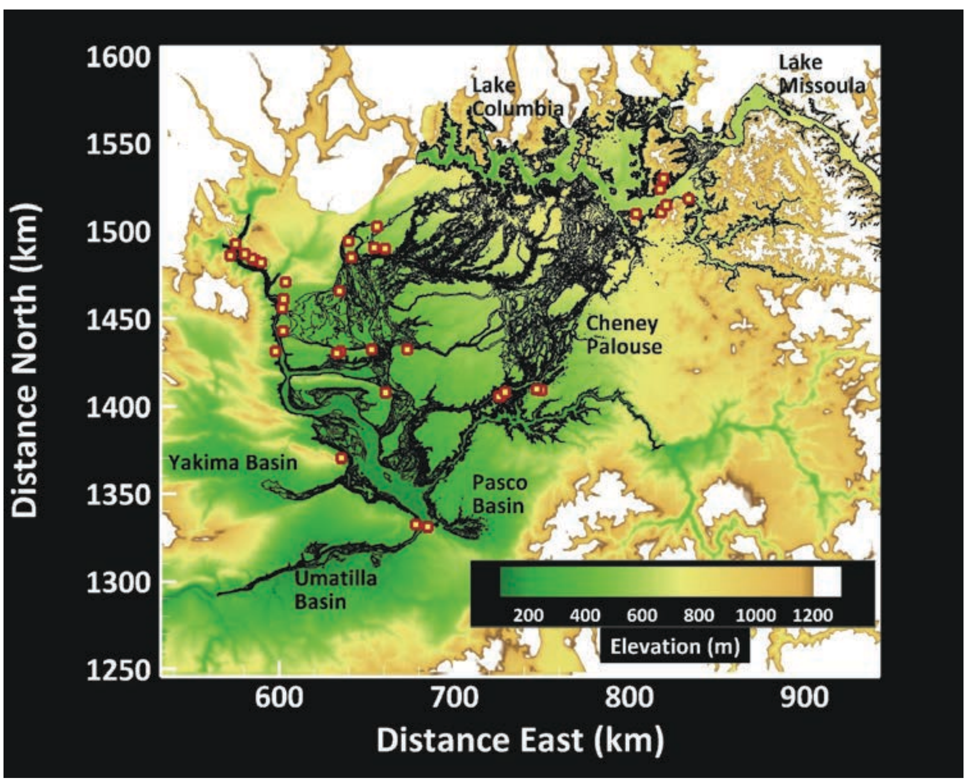

Figure 4. Flood paths in eastern Washington obtained by contouring flow margins of our scenario 1b output 23 h after dam break. Also shown are the field data control points used in this paper and listed in Table 1. Grid and terrain map produced with an Albers projection with a NAD 1983 reference. Part of Lake Missoula and all of Lake Columbia show up well in this image. All elevations above 1200 m, the northern portions of which represent Cordilleran ice, block dam-break flows and are shown in white in this image.

have been deposited during a flood declining from its maximum stage. However, the presence of numerous such elements—for instance, many ice-rafted erratics at similar elevation in an area—strengthens their constraint as an upper bound on flood stage. Scabland erosion is an indirect, weak constraint on depth that only indicates erosive flow. A strong constraint exists where definitive flood erosion occurred in an area where similar landscape elements that remained uneroded are found nearby.

METHOD OF ANALYSIS

Model Surface Construction

We simulated floods using a digital model of the topography, or grid, of the entire Columbia River drainage from western Montana to the sea and from southern Canada to central Oregon, and the grid resolution determined how closely we could compare model results to field data. This grid was constructed from U.S. Geological Survey (USGS) digital elevation models at a 30 m posting using an Albers (equal-area) projection, North American Datum of 1983. Whereas a 30 m mesh could be constructed for better resolution of flow, practical considerations of computer processing time resulted in decimating the 30 m grid to 185 m. Only relevant parts of the computational grid are shown in this report, though the entire grid extending over southern British Columbia and Alberta, all of Washington, and half of Oregon was used in calculating model flows. Existing large dams on the Columbia and Snake Rivers were removed, and available bathymetry was used to reconstruct the missing topography. The result is shown in Figure 1, with the Cordilleran ice sheet and all elevations above 1200 m that blocked flow are shown. The ice-sheet terminus was found from published reports (Waitt and Thorson, 1983; Waitt et al., 2016). The terminus for the Okanogan lobe near the entrance to upper Grand Coulee, and blockage of the entrance to upper Grand Coulee varied with each scenario as described below. The accuracy of the field evidence is limited by the method used to obtain elevations. In many cases, topographic maps were used to map deposits, yet the model was run on a digital model of the terrain. The local uncertainty between elevations on the 7.5 min topographic maps used to locate the data and the elevations on the numerical grid built from the USGS topographic database is presented later in this report.

Model Description

We used the open-source software package GeoClaw (www.clawpack.org) to calculate depth-averaged flow on the digital model we constructed of the three-dimensional terrain. This software employs shock-capturing, finite volume methods and conservative numerical schemes (LeVeque, 2002) that balance mass and momentum. GeoClaw features advanced numerical schemes (Berger et al., 2011) that were developed to more accurately capture flood fronts inundating dry land as they move over variable terrain (George, 2008, 2011).

Model Initial and Boundary Conditions

To simulate initial conditions for rupture of an ice dam blocking glacial Lake Missoula, the Purcell Trench lobe was modeled as an ice tongue that dammed the Clark Fork River to form glacial Lake Missoula, as shown in Figure 5. In some scenarios, the Okanogan lobe also blocked the Columbia River downstream, creating Lake Columbia, also as shown in Figure 5. The Lake Missoula ice dam was then suddenly removed to initiate a dam-break flow. An instantaneous release condition is common in dam-break simulations (Abril-Hernández et al., 2018; Alho et al., 2010; Bohorquez et al., 2016), though Alho et al. (2010) artificially imposed a hydrograph input downstream, presumably near the outlet but in the Rathdrum channel, to model inundation. In our model, the configuration of the ice dam and the instantaneous removal scheme were the same for all scenarios, as they were in all our previous work.

For the Missoula floods, a sudden or very rapid dam-break simulation, in contrast to a slow release of water from the dam, is supported by field data (Alho et al., 2010). Given the rugged topography around the dam-break site and along the Rathdrum valley to Spokane, rapid dam failure must occur when the stage behind the dam is high enough to achieve the high flow stages observed in and around Spokane (Fig. 1). A drainage of any duration, whether weeks, months, or years, is not supported by field data if it caused significant drainage of the lake volume. If the volume of water bleeding out of a progressive rupture of the ice dam is insignificant relative to the volume of water in Lake Missoula, then regardless of how long it takes to cause catastrophic rupture of the ice dam, the stage at the dam site does not drop much. Once the dam catastrophically fails, the dam-break discharge is determined by the stage behind the dam, and the time it took to fail is irrelevant.

Once catastrophic failure of the ice dam occurs, the shape of the initial flood wave at the dam is determined by the stage behind the dam and the bathymetry of the lake. The depression wave that progresses upstream from the dam-break site, and the interaction of that wave with topography determines the flooding downstream from the dam site. As flow continues, the physics of depth-averaged flow would produce a flood wave that increasingly broadens with time as it moves downstream. In calculating resulting dam-break flows for this report, we greatly improved flow-front accuracy over rugged topography and model efficiency with the use of adaptive mesh refinement (AMR), as described in George (2011). Whereas all dam-break wave velocities are calculated in the same way as in Denlinger and O'Connell (2010), the many details in the terrain are captured here by much smaller cell sizes along the flow fronts, while decreasing computation times from months to days with the use of AMR. This increased accuracy provides a lot of confidence in our assessments, particularly for the innumerable channels in the complex Cheney-Palouse terrain, as our cell size was refined dynamically to minimize inundation errors. This desirable feature was not present in the model of Denlinger and O'Connell (2010).

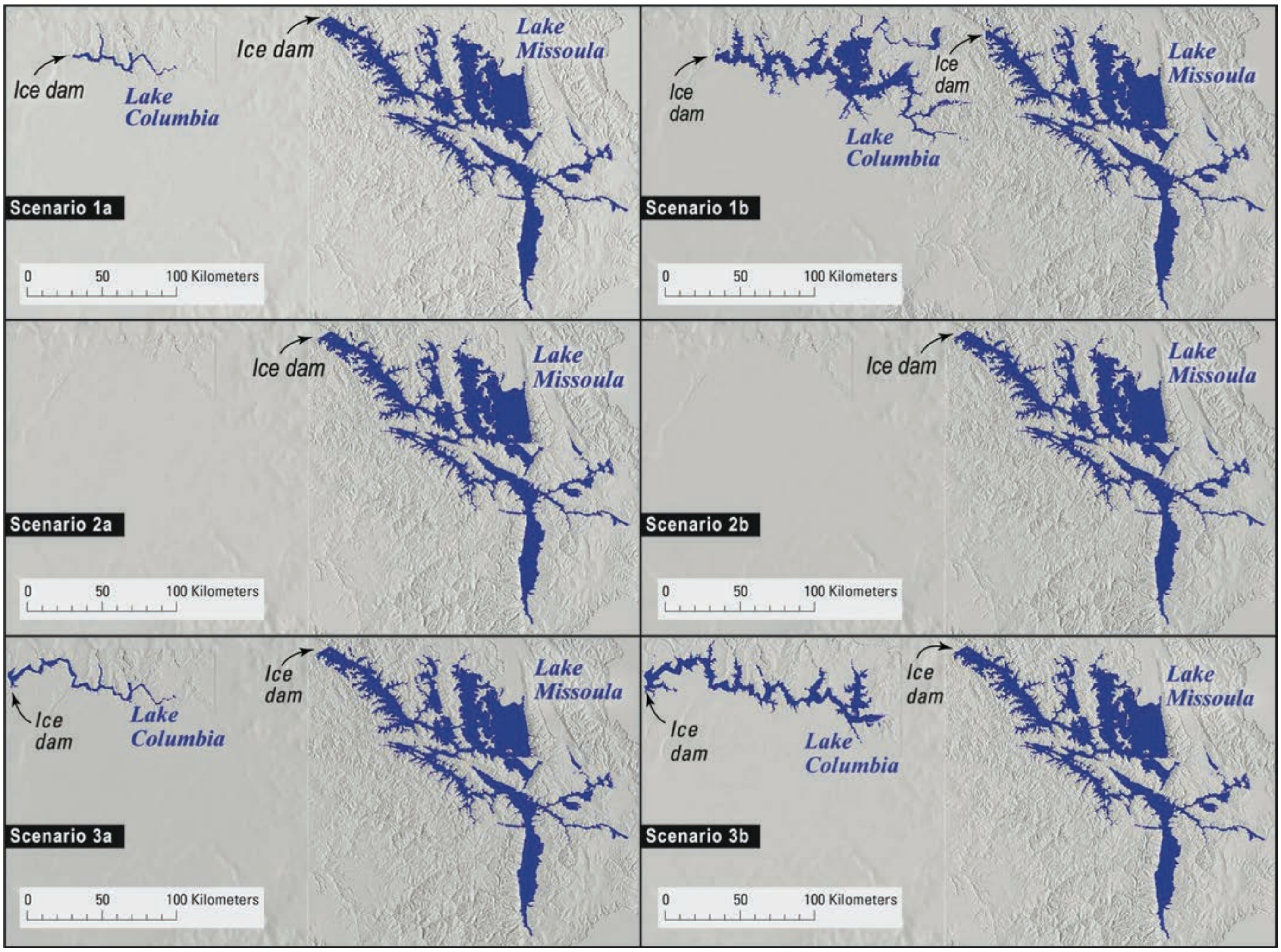

Figure 5. Comparison of initial conditions of Columbia River valley blockage and blockage of upper Grand Coulee for each of the six scenarios tested in this report. The stage in Lake Missoula is at an elevation of 1265 m. Blockages of the Columbia River valley create a Lake Columbia in scenarios 1a, 1b, 3a, and 3b, and the existence of this lake interacts with the dam-break flow to create a seiche that influences flooding. The two scenarios with an open channel, 2a and 2b, have the longest route and produce the slowest floods and the lowest flood stages on their way from Spokane to Umatilla. The most rapid flows and highest stages occur with scenarios 1b and 3b.

FLOOD MODELS

Scenarios for Flooding

Given current topography, no single position of the Cordilleran ice margin will flood all the pathways for which there is abundant evidence for flooding (Fig. 4; Table 1). As a consequence, we chose to investigate a spectrum of six solutions for flooding in eastern Washington. These six scenarios were defined by six combinations of blockages of Columbia River valley and upper Grand Coulee by ice or rock, as described below.

Six distinct blockages forming modeling scenarios, labeled 1a to 3b, produced six different inundation patterns during flooding. There were two controlling factors: (1) the extent of the Okanogan ice lobe that blocked the Columbia River valley, and (2) the existence of a blockage of upper Grand Coulee (by either rock or ice). These two controlling factors have been long identified as key factors in understanding Missoula flood dynamics downstream near Quincy Basin (Hanson, 1970; Waitt and Thorson, 1983; Atwater, 1987; Waitt et al., 2009; Waitt, 2016). Here, we chose three Okanogan lobe positions coupled with either an open or closed (blocked) upper Grand Coulee to produce the six model scenarios. Initial conditions for each scenario are illustrated in Figure 5 and described as follows.

Scenario 1a

In scenario 1a, the Okanogan lobe is at its maximum extent and blocks the Columbia River valley west of the intake to upper

Grand Coulee, but upper Grand Coulee is open and incised to its present depth. This scenario implies a low-level glacial Lake Columbia that still drains over the 471 m floor elevation of upper Grand Coulee.

Scenario 1b

The Okanogan lobe is at its maximum extent and blocks the Columbia River valley, and rock or ice blocks upper Grand Coulee. The Grand Coulee blockage is high enough to produce a stage of 685 m for glacial Lake Columbia, based on the elevations of potential spillover terrain adjacent to the upper Grand Coulee channel. This condition forms the largest, most extensive glacial Lake Columbia of all scenarios tested. The blockage forces all flow through the Cheney Palouse and Telford tracts draining southwest into Quincy Basin and results in the shortest flood paths to Quincy and Pasco Basins.

Scenario 2a

The Okanogan lobe does not encroach into the Columbia River valley, which remains open. This scenario is supported by field evidence for large Missoula floods down the Columbia River valley (Waitt et al., 2009; Waitt, 2016) near Wenatchee, and it allows floodwater access to Moses Coulee. There is no glacial Lake Columbia.

Scenario 2b

As in 2a, the Columbia River valley is ice free, allowing floodwaters access both to the Columbia River valley and Moses Coulee. In contrast to 2a, access to the upper Grand Coulee channel from the Columbia River valley is blocked by rock. This assumes that the upper cataract in Grand Coulee has not yet eroded northward to the Columbia River valley. As for scenario 1b, the divide crossing associated with upper Grand Coulee is reconstructed to be 685 m elevation.

Scenario 3a

Here, the Okanogan lobe blocks the Columbia River valley west of Moses Coulee, but it allows floodwater to enter into Moses Coulee itself. This results in a smaller glacial Lake Columbia with a stage maintained by the 465 m floor elevation of upper Grand Coulee.

Scenario 3b

The Okanogan lobe blocks the Columbia River valley while rock blocks the upper Grand Coulee channel to an elevation of 680 m. This topography forces glacial Lake Columbia to drain through Moses Coulee during a large Missoula flood.

RESULTS

The six scenarios described here create distinctly different flood routings between Spokane and Pasco Basin that result in significant variations in the amount and rate of filling of Pasco and Umatilla Basins, as flood waters become temporarily dammed by slow flow through Columbia River Gorge. The dynamics of depth-averaged flow in models for surface flow of water produced a consistent pattern: The longer flow paths across eastern Washington resulted in more area flooded between the ice dam and Pasco Basin and Umatilla Basin, and a longer time to fill these large basins.

For all scenarios catastrophic flooding of eastern Washington filled Pasco and Umatilla Basins at different rates, yet these rates were nearly a hundred times faster than the time to drain these great basins through Columbia River Gorge. Dynamic flow modeling clearly shows that Columbia River Gorge was the primary bottleneck in the entire flow path from the ice dam to the sea. As a result of its location in the entire drainage path, the longer it took to fill Yakima, Pasco, and Umatilla Basins, the more drainage there was through the Columbia River Gorge as these basins were filling, and the lower the maximum stage in these basins was for any given scenario. Of all six scenarios tested, scenario 1b filled Pasco basin the fastest and achieved the highest stages in all three basins (Fig. 6). Scenarios 2a, 2b, 3a, and 3b had more channels open than scenarios 1a and 1b, had larger areas of inundation, and thus had lower water surface slopes and slower velocities. As a consequence, these latter scenarios filled Yakima, Pasco, and Umatilla Basins at the slowest rate (Fig. 7). The scenarios with the smallest inundation area and the shortest paths from Spokane to Columbia River Gorge (scenarios 1a and 1b) produced the most rapid flooding and the highest simulated flood stages observed (Fig. 8).

These differences in flooding for each scenario are supported by field data. When ice blocked the Columbia River valley to form glacial Lake Columbia, a distinctive pattern of flooding formed (Fig. 6), and this showed that a large glacial Lake Columbia would have resulted in inundation of the entire Telford scabland tract shown to have flooded in Figure 3. In the simulations, the higher the ice blockage of the Okanogan lobe, the larger glacial Lake Columbia becomes, and the greater is the discharge into the Telford and Cheney Palouse scabland tracts when a Missoula flood occurs. The largest flow through Telford tract, and the only one that fits all scabland scars indicated by the image in Figure 3, only occurred with the maximum blockage scenario 1b. All other scenarios produced smaller glacial Lake Columbia volumes (Fig. 5) and did not produce flood stages high enough to flood all Telford scablands.

When the Columbia River valley was not blocked by the Okanogan lobe, the flood scenarios here formed another unique set of solutions. The two scenarios that have an open Columbia River valley channel, 2a and 2b, flooded the entire channel from Spokane to Wenatchee. Along this channel, flow southward and downstream at Wenatchee formed giant ripples on Pangborn bar at Wenatchee that cannot have been formed by more passive backflooding upstream as water backed up the Columbia River valley channel from the south. Nearby erratics indicate a minimum floodwater stage of 490 m there (Table 1), but they do not distinguish direction of flow. Though flow solutions for 2b achieved a maximum stage of 455 m at Wenatchee, this value is still 35 m below the field evidence given by erratics for the highest flood stage at Wenatchee (Table 1). Scenario 2a, with water diverted from the channel into an open upper Grand Coulee upstream, had a lower discharge at Wenatchee that simulated flood stages tens of meters lower across Pangborn bar than scenario 2b.

The other major difference between the open Columbia scenarios 2a and 2b is revealed by the flooding of Quincy Basin. As shown by the snapshot in Figure 8A, when upper Grand Coulee is open (scenario 2b), Quincy Basin is already flooded from the east 23 h after dam break. If upper Grand Coulee is blocked (scenario 2a), then Quincy fills more slowly, fills later, and fills mainly from the west. Field evidence for both scenarios exists (Waitt, this volume), providing evidence that these two different initial conditions existed at the onset of different floods.

DISCUSSION

There are systematic differences between simulated maximum model stage and the maximum stage constrained by field data across the entire drainage area from Spokane to Pasco Basin. These differences not only support separate initial conditions for separate floods, but they also suggest that the volume of floodwaters was enhanced during flooding. The field sites listed in Table 1 are shown in Figure 9, along with their uncertainty in elevation, and the flooded contours of differences between the maximum stage obtained by any model at the nearest point to a field site and the maximum elevation of field data at that site.

Elevation errors in field data are random and have an approximate Gaussian distribution relative to the elevations on the

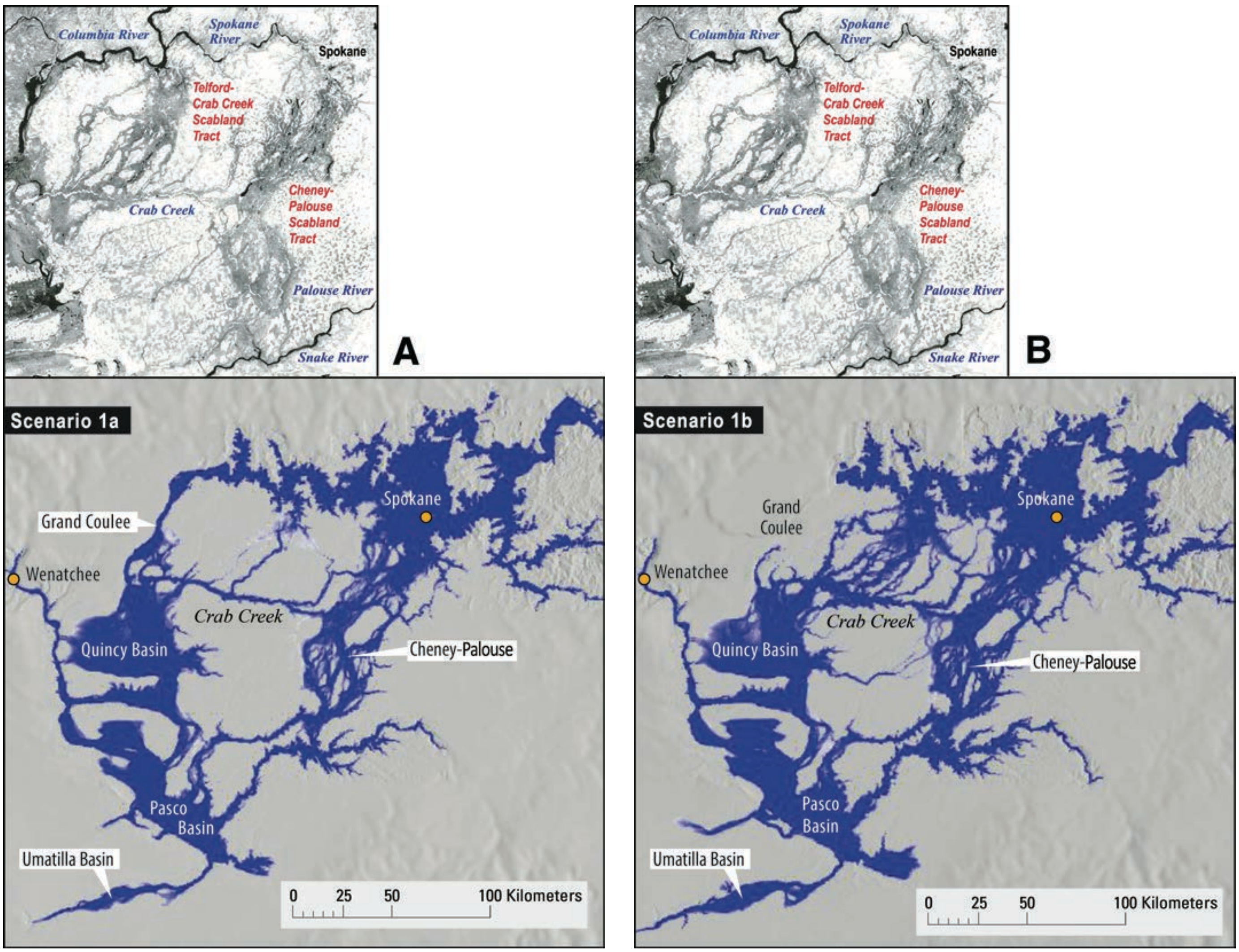

Figure 6 (*Continued on following page*). Scenarios 1a, 1b, 3a, and 3b at 23 h after dam break: (A) scenario 1a; (B) scenario 1b; (C) scenario 3a; and (D) scenario 3b. All flood Telford scabland. Only scenario 1b produces the broad extent of scarring visible in the satellite image above. Flooding of Telford scabland tract requires that the Columbia River valley is blocked, and maximum flooding of Telford scabland only occurs when flow into upper Grand Coulee is blocked.

digital grid on which we simulated flooding. The digital terrain model used here has more precise topographic control, despite being a compilation of different spatial data, and it is far more accurate than the elevations obtained from field site locations on 7.5 min topographic maps (regardless of how well the point is located on the map). A histogram of the differences between field site elevations and our digital terrain model is shown in Figure 9B. The discrepancies approximate a Gaussian error model with a standard error of ~5 m, indicating that errors are random and that meaningful differences between model and field data for stage should be at least 10 m. Many of the model versus field stage discrepancies that we obtained from our model simulations are tens of meters at each field location (Table 1), indicating that these differences are significant.

Other sources of error include model errors and landscape modification during flooding. For model errors, the simulation of the Malpasset dam break (George, 2011), with precise timing and location of inundation recorded along the flow path, showed that model errors resulting from either the shallow-water flow approximation or the flow calculation method are insignificant relative to field errors for sudden release of a known volume from a dam. Erosion of the terrain, particularly during bulking by loess, is a significant source of inundation error in the Cheney-Palouse scabland, but we are calculating flow on the eroded terrain, so the error is included once erosion has occurred and substrate volume is incorporated into the floodwaters. The main effect of this bulking will be increased flood stages downstream of the locations where this erosion occurs.

There were systematic variations in the differences between our simulated model stages and elevations at the field sites across eastern Washington, increasing southwestward from Spokane to Pasco Basin (Table 1; Fig. 9C). Maximum model stages exceed the field evidence by 20 m to 30 m or more at Spokane and match field data along much (and probably all) of the northern reach

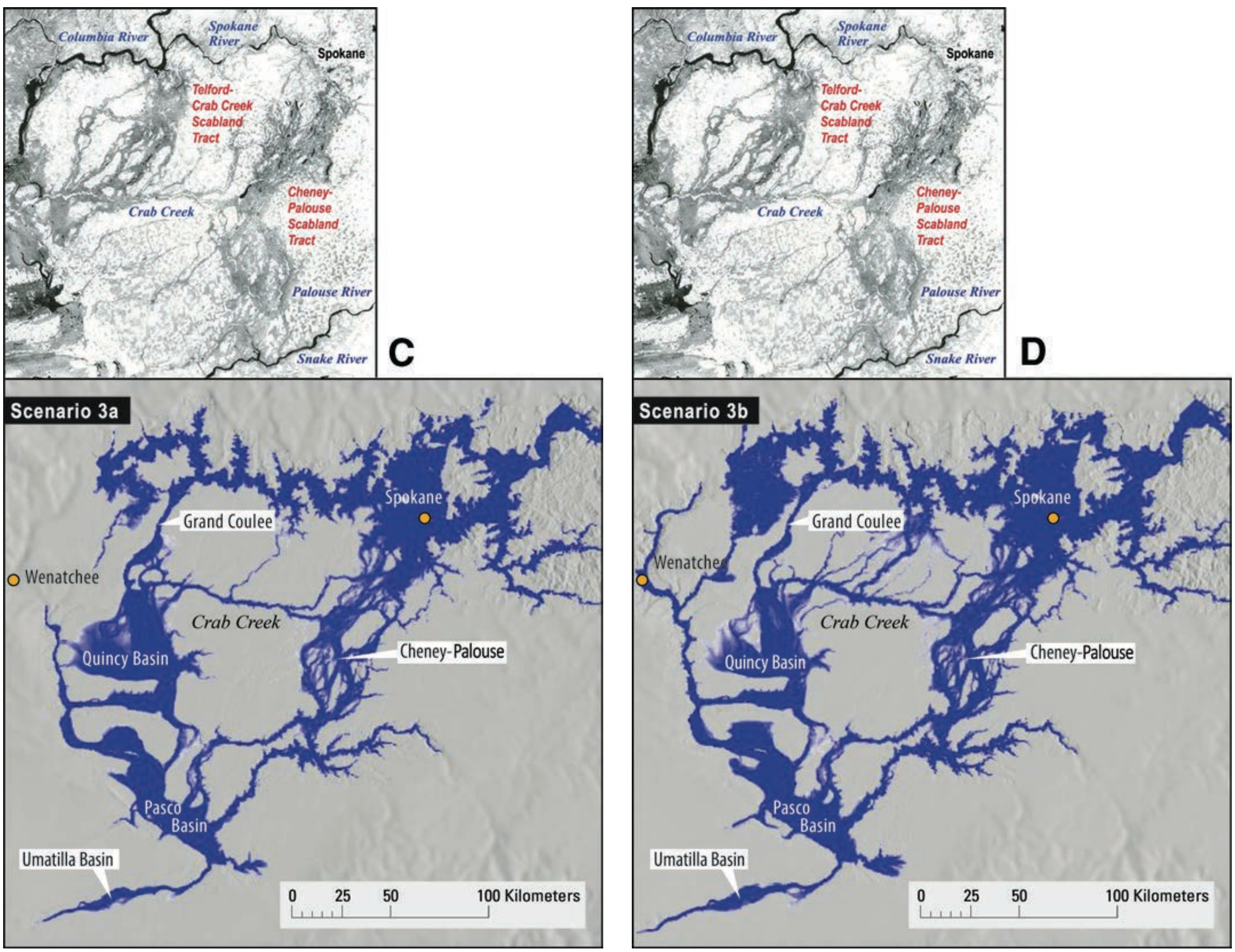

Figure 6 (*Continued*).

of the Columbia River valley to the entrance of upper Grand Coulee, but systematically fall short of field-determined stages along the drainage paths (mainly in the Cheney Palouse and Telford tracts) toward Pasco Basin. Along other drainage paths, maximum model stages (relative to field data) are deficient by 35 m at Wenatchee, and by at least 40 m in Quincy and Pasco Basins (Fig. 9C). These differences show that either additional sources of flood volume (such as incorporation of eroded loess) or another source of water other than glacial Lake Missoula contributed to these floods. If these floods had been augmented by significant flow from a source farther north, as Shaw et al. (1999) suggested, then this combined flow would have had to pass northern field sites where modeled flood stages exceeded maximum field-determined stages. Thus, our modeling results show that an additional glacial source of floodwater north of Columbia channel is not supported by this study. We consider two alternatives to supply excess volumes below.

Alternative sources of flow volume that can remove the model–field stage discrepancies are either release of glacial Lake Columbia during a Missoula flood, or bulking of floodwaters by windblown loess. For the first possibility, failure of the ice dam blocking glacial Lake Columbia could have been triggered by a rapidly increasing stage from a Lake Missoula dam break upstream. Our results show that a Lake Columbia ice-dam failure is the most likely source to explain the large negative model versus field stage discrepancies at Wenatchee. However, this secondary dam rupture flows mostly toward Wenatchee, and cannot have produced the flooding that generates negative model-field stage discrepancies across the Telford and Cheney-Palouse tracts. Somewhere along these tracts, the discrepancies between

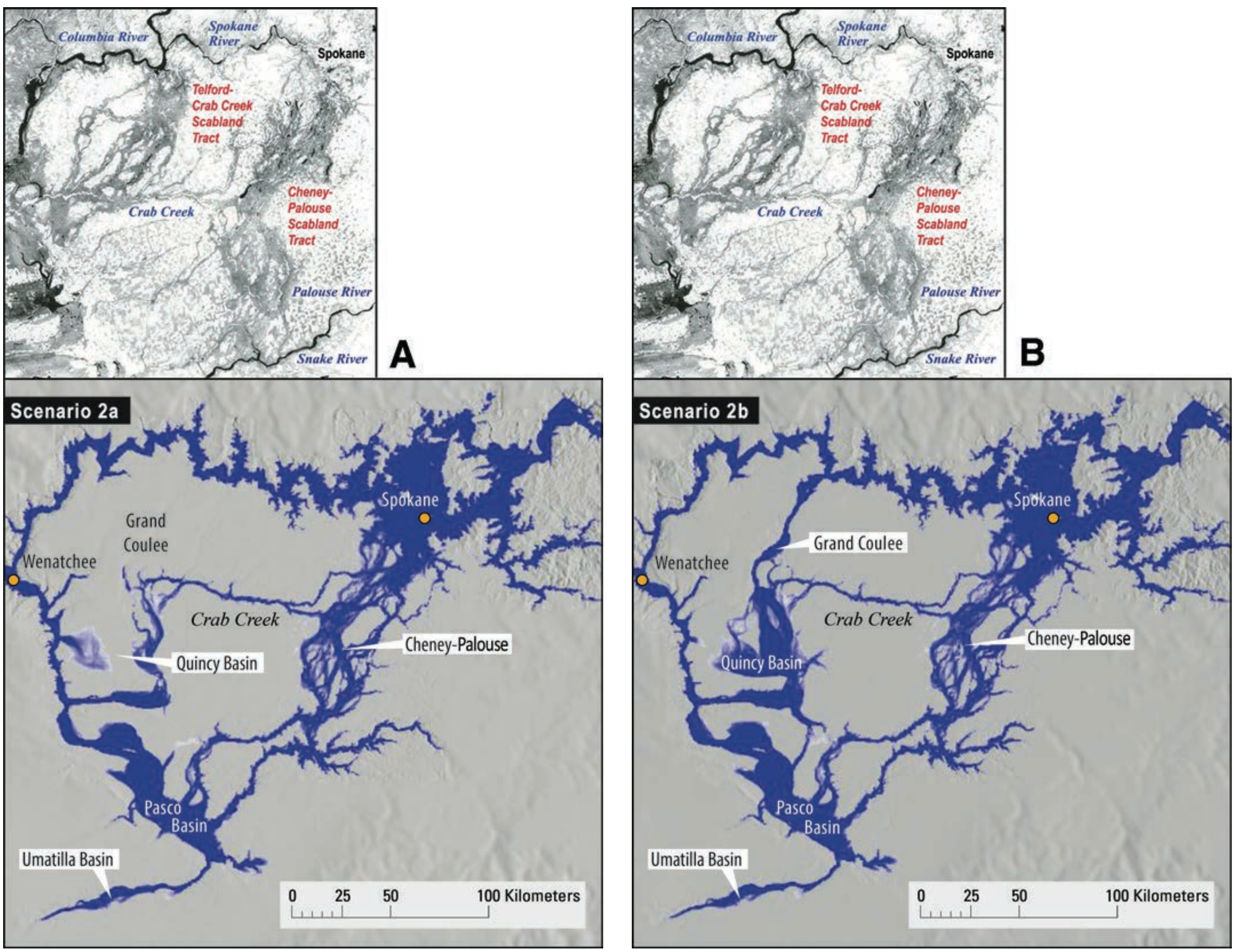

Figure 7. Scenarios 2a and 2b at 23 h after dam break: (A) scenario 2a and (B) scenario 2b. The two scenarios, in which the Columbia River valley is open, are required to match the field evidence for high water and erosion of Pangborn bar, the giant point bar forming the big bend in the Columbia River at Wenatchee. Scenario 2a floods Quincy Basin from the east; scenario 2b floods Quincy Basin from the west.

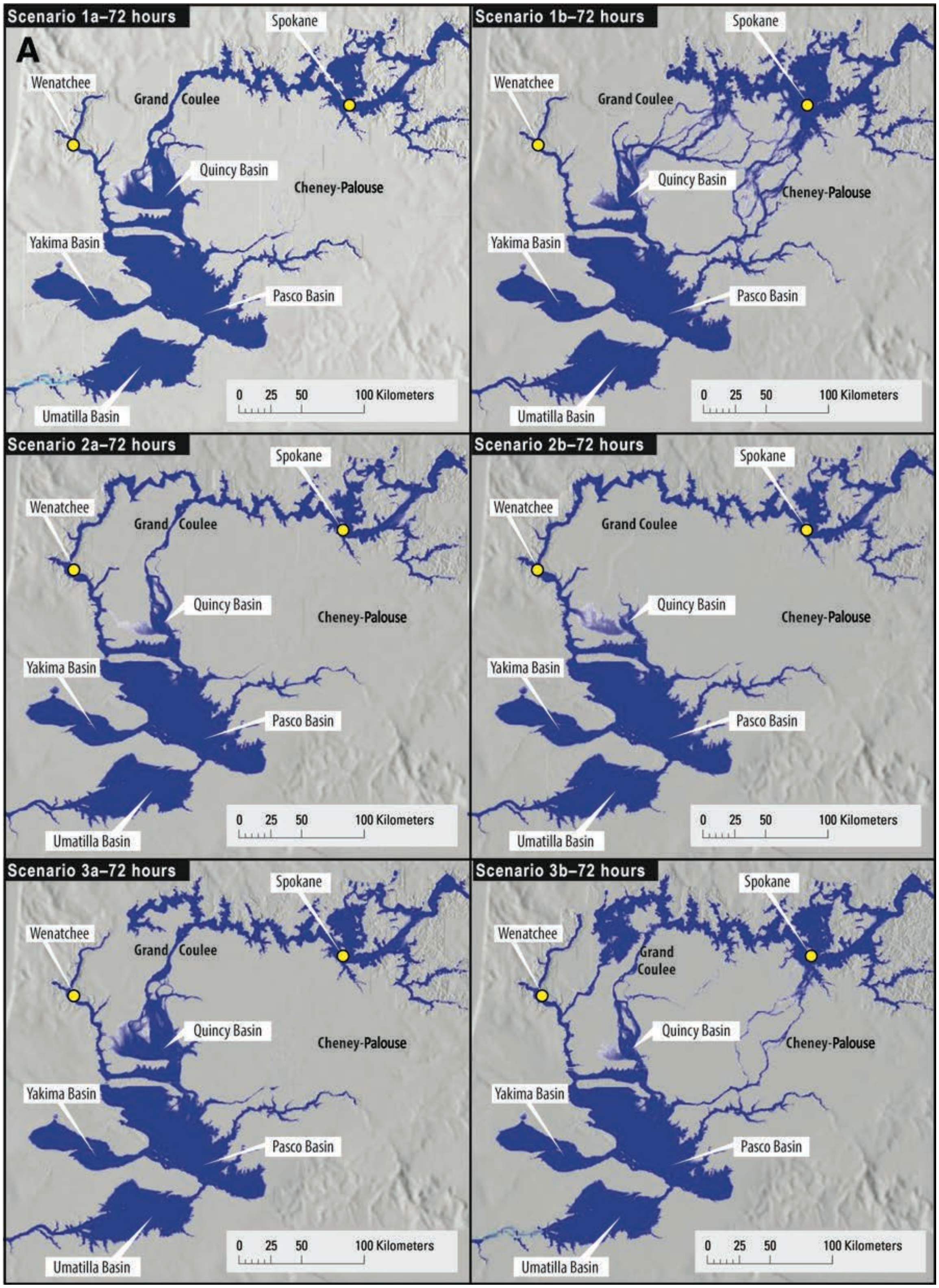

Figure 8 (*Continued on facing page*). (A) All scenarios 72 h after dam break, when flooding in each scenario is close to maximum stage in the large basins of Pasco, Umatilla, and Yakima. The variations in flooding between scenarios result from variations in the route taken to these basins. Between 72 h and 80 h, the stage in each basin begins to decline. Complete drainage of these basins through Columbia River Gorge takes many weeks.

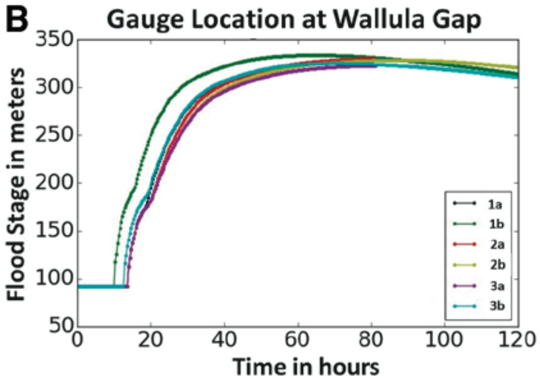

Figure 8 (*Continued*). (B) Variation in the rate of filling of Pasco and Umatilla Basins for each scenario tested, as determined with a model gauge location at Wallula Gap. Maximum stage is achieved first by scenario 1b at about 60 h, whereas 72 h is required for scenarios 1a, 2a, 2b, 3a, and 3b. Compare these results with the different paths taken as shown in Figures 6 and 7.

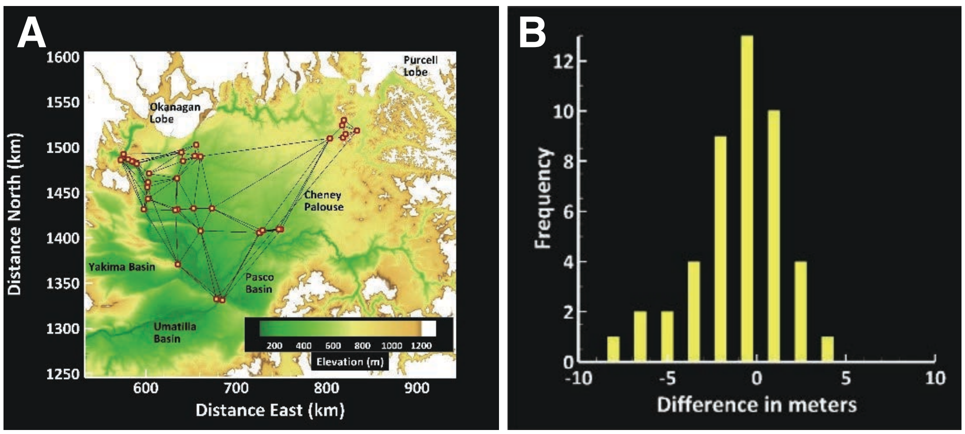

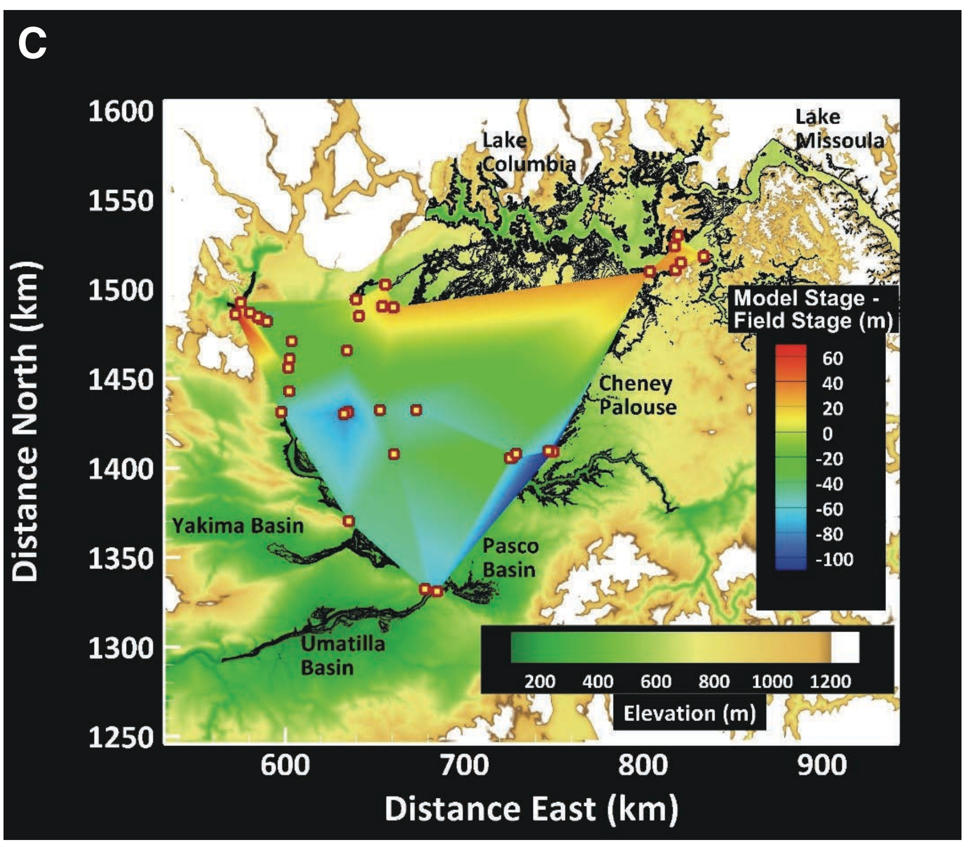

Figure 9. (A) The topography of the drainage basin with the locations of field control points used in this study and listed in Table 1. (B) Discrepancy between the field elevations and the elevations on the digital surface used to route floods. (C) Differences between the maximum model stage and the maximum field stage in an ensemble in which all scenarios are equally likely. All model flows exceed field evidence by more than 30 m near Spokane and along the Columbia River valley to the entrance of upper Grand Coulee, and values match indicators within Moses and Grand Coulees. However, all model flows are deficient by about 20 m at Pangborn bar at Wenatchee and are more than 40 m below high-water indicators downstream in Quincy and Pasco Basins. The erosion of loess, which creates the dark channel–light loess pattern in Figure 3, is the most likely volume source in the Telford and Cheney-Palouse scablands, but deficiencies near Wenatchee may indicate release of glacial Lake Columbia.

the model and the field data reverse: Though model flood stages are higher than field data stages in Spokane, they are lower than field data stages in the lower Cheney Palouse and in Pasco Basin. The most likely volume source to reverse the more than +40 m model field discrepancies across the Cheney Palouse and Telford tracts is bulking of floodwaters by erosion and incorporation of thick deposits of windblown loess.

Evidence for bulking of floodwaters by loess is represented by residual plateaus of loess, remnants left by passage of these floods (Fig. 2C). Windblown loess will be carried away by surging floodwaters as suspended load and will be kept in suspension nearly indefinitely by turbulence within the flow. Scabland scars surround each of the 35-m-high, teardrop-shaped islands of loess (Fig. 2C), and the shape and sculpting of each island indicate flow north to south during their formation. The eroded loess contributed to large volumes of fine sediment deposits (~10–50 mm; Higgins et al., 1985) in slack-water areas such as Burlingame Canyon (Fig. 2D) and produced huge volumes of sediment offshore (Normark and Reid, 2003).

Only a fraction of the volume of loess eroded from the scablands is sufficient to reverse our model versus field discrepancies along drainage paths between Spokane and Pasco Basin. The actual erosion will be calculated in subsequent work, but we tested to see if the volumes were sufficient to erase model-field stage discrepancies. The drainage paths for the most voluminous flows across the Cheney-Palouse scabland (scenario 1b) are shown in Figure 10. If a loess thickness of 35 m (Higgins et al., 1985) is assigned along the rust-colored flood channels in the Telford and Cheney Palouse scabland tracts in Figure 10, then removal of that loess volume bulks the flow and produces more flow volume. With our model flood, we removed all loess along a drainage path, and then we used this increased volume to determine the higher stage in Quincy and Pasco Basins. We found that removal of all loess in each channel in a single flood for scenario 1b would produce stage increases in both Quincy and Pasco Basins that greatly exceed our model versus field stage discrepancies. Only a fraction of the volume of eroded loess is needed to remove the model–field stage discrepancies. Though each flood may have eroded loess, it is likely that one of the largest early floods eroded the most loess and produced the model–field stage discrepancies observed. These stage increases from loess removal include subsequent drainage of the Quincy Basin volume into Pasco and Umatilla Basins. The windblown loess, in the highly turbulent floodwaters, could have been kept in suspension for weeks by these high-energy flows as turbulence was continuously regenerate by flow. Consequently, much of the eroded loess would have remained in suspension and been transported out to sea to form deposits observed on the seafloor (Normark and Reid, 2003).

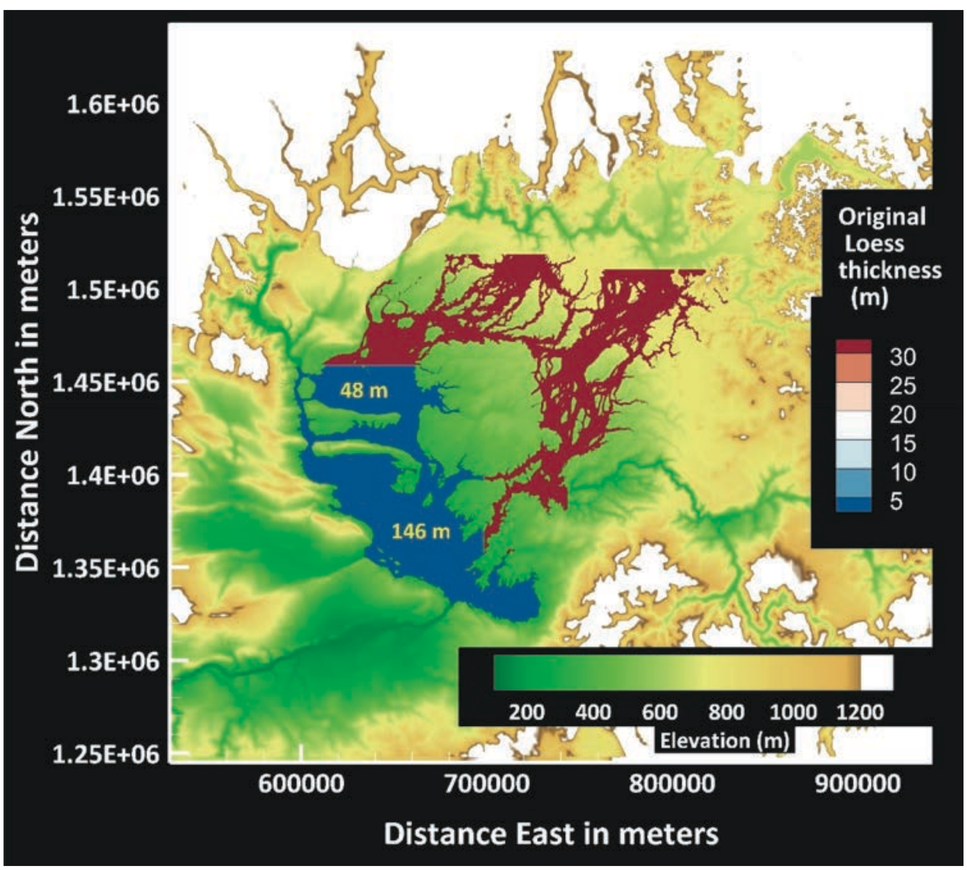

Figure 10. Consequence of removal of 35 m of loess from the rust-colored channels in a single flood will produce stage increases in Quincy and Pasco Basins that vastly exceed the deficiencies between observed stage and model stage, shown as yellow numbers here. In Pasco Basin, there is an increased volume as the suspended load in Quincy Basin drains into Pasco Basin, because this occurs in one day, whereas drainage of Pasco Basin takes weeks. These stage increases are two to three times that required to erase statistically significant discrepancies between the field and model data in Quincy and Pasco Basins. However, the veracity of such drastic bulking needs to be tested with a dynamic model for erosion, transport, and deposition. Grid and terrain map produced with an Albers projection with a NAD 1983 reference.

CONCLUSIONS

Research on the Missoula floods has documented field data that were used to inform sophisticated depth-averaged flow models for these large floods. Here, we utilized a digital terrain model with a 185 m posting (points spaced equally at 185 m N-S and E-W), with existing large dams removed, and a continental ice sheet added to the topography of eastern Washington in late Wisconsin time. Field evidence shows both flooding of multiple channels and dozens of floods, yet all channels cannot have been occupied for any given position of the Cordilleran ice sheet terminus up to its maximum extent. We constructed three Okanogan lobe conditions coupled with either an open or closed upper Grand Coulee to produce six representative scenarios, each with a different history of inundation. By comparing flood stages for each scenario with field data, we determined that:

(1) The flood scars that are captured in detail on large-scale topographic maps (and also visible in Landsat images) in the Telford scabland tract require both the maximum extent and volume of glacial Lake Columbia and the maximum glacial Lake Missoula at the time that Purcell Trench ice lobe impounding Lake Missoula failed. Failure of both a smaller blockage of the Columbia River forming glacial Lake Columbia and a smaller blockage of glacial Lake Missoula does not have the volume required to flood and produce all of the channel erosion observed.

(2) Maximum flood stage indicated by ice-rafted erratics near Wenatchee requires a dam-break scenario in which ice did not block the Columbia River valley, but in which the entrance into upper Grand Coulee was blocked, presumably by rock. This difference in channel blockage also would have affected subsequent flooding downstream: With upper Grand Coulee blocked, Quincy Basin floods first from the west, whereas if upper Grand Coulee is open, Quincy Basin floods first from the east. As there is field evidence for both flooding scenarios, two different initial conditions occurred during separate Missoula floods.

(3) Each dam-break failure of Lake Missoula in the model floods drains eastern Washington over a period of three to four days, producing peak flood stages in Pasco and Umatilla Basins (including Wallula Gap) between 60 h and 72 h after a catastrophic dam break occurs. Floodwaters are stored in Umatilla, Pasco, and Yakima Basins because drainage through Columbia River Gorge takes weeks. For scenario 1b, the flooding agrees both in inundation patterns and timing with the previous study by Denlinger and O'Connell (2010).

(4) Discrepancies between modeled flood stages and field evidence among various scenarios show that blockage of both the Columbia River valley by the Okanogan lobe and upper Grand Coulee by rock or ice is required to produce the highest discharge across eastern Washington, and gives the maximum modeled flood stages in Pasco and Umatilla Basins. This is a result of these blockages producing the shortest floodwater paths between Spokane and Pasco Basin, which results in the most rapid drainage of eastern Washington.

(5) Discrepancies between modeled flood stages and field evidence for maximum flood stages show a systematic variation north to south across eastern Washington: Model stages are consistently higher than field stages near Spokane, about equal along the Columbia River valley from Spokane to upper Grand Coulee, and consistently much lower than field stages in Quincy and Pasco Basins and in Columbia River Gorge. Erosion of vast quantities of loess from the Telford and Cheney Palouse scabland tracts is a plausible source of increasing and systematic deficiencies in simulated flood volume as the floods traverse scabland tracts. Significantly, only a small fraction of this eroded sediment from these uplands is required to bulk model floods enough to eradicate model-field discrepancies in Pasco Basin, but erosion of loess on these paths cannot explain the model versus field stage discrepancies at Wenatchee. Discrepancies in model versus field stages at Wenatchee suggest that concomitant dam failure of a large glacial Lake Columbia could have augmented some of these dam-break floods.

ACKNOWLEDGMENTS

The U.S. Geological Survey funded this research.

REFERENCES CITED

Abril-Hernández, J., Perianez, R., O'Connor, J., and Garcia-Castellanos, D., 2018, Computational fluid dynamics simulations of the late Pleistocene Lake Bonneville flood: Journal of Hydrology (Amsterdam), v. 561, p. 1–15, https://doi.org/10.1016/j.jhydrol.2018.03.065.

Alho, P., Baker, V.R., and Smith, L., 2010, Paleohydraulic reconstruction of the largest glacial Lake Missoula draining(s): Quaternary Science Reviews, v. 29, p. 3067–3078, https://doi.org/10.1016/j.quascirev.2010.07.015.

Atwater, B.F., 1984, Periodic floods from glacial Lake Missoula into the Sanpoil arm of glacial Lake Columbia, northeastern Washington: Geology, v. 12, no. 8, p. 464–467, https://doi.org/10.1130/0091-7613(1984)12<464:PFFGLM>2.0.CO;2.

Atwater, B.F., 1986, Pleistocene Glacial-Lake Deposits of the Sanpoil River Valley, Northeastern Washington: U.S. Geological Survey Bulletin 1661, 39 p.

Atwater, B.F., 1987, Status of Glacial Lake Columbia during the last floods from glacial Lake Missoula: Quaternary Research, v. 27, p. 182–201, doi:10.1016/0033-5894(87)90076-7.

Baker, V.R., 1973, Paleohydrology and Sedimentology of Lake Missoula Flooding in Eastern Washington: Geological Society of America Special Paper 144, 79 p.

Benito, G., and O'Connor, J.E., 2003, Number and size of last-glacial Missoula floods in the Columbia River valley between the Pasco Basin, Washington, and Portland, Oregon: Geological Society of America Bulletin, v. 115, p. 624–638, https://doi.org/10.1130/0016-7606(2003)115<0624:NASOLM>2.0.CO;2.

Berger, M.J., George, D.L., LeVeque, R.J., and Mandli, K.T., 2011, The GeoClaw software for depth-averaged flows with adaptive refinement: Advances in Water Resources, v. 34, p. 1195–1206, https://doi.org/10.1016/j.advwatres.2011.02.016.

Bohorquez, P., Carling, P., and Herget, J., 2016, Dynamic simulation of catastrophic late Pleistocene glacial-lake drainage, Altai Mountains, central

Asia: International Geology Review, v. 58, p. 1795–1817, https://doi.org/10.1080/00206814.2015.1046956.

Bretz, JH., 1923, The Channeled Scabland of the Columbia Plateau: The Journal of Geology, v. 31, p. 617–649, https://doi.org/10.1086/623053.

Bretz, JH., 1925, The Spokane flood beyond the Channeled Scabland: The Journal of Geology, v. 33, p. 97–115, https://doi.org/10.1086/623179.

Bretz, JH., 1928a, Bars of the Channeled Scabland: Geological Society of America Bulletin, v. 39, p. 643–701, https://doi.org/10.1130/GSAB-39-643.

Bretz, JH., 1928b, The Channeled Scabland of eastern Washington: Geographical Review, v. 18, p. 446–477, https://doi.org/10.2307/208027.

Bretz, JH., 1929, Valley deposits immediately east of the Channeled Scabland of Washington, 1: The Journal of Geology, v. 37, p. 393–427.

Bretz, JH., 1969, The Lake Missoula floods and the Channeled Scabland: The Journal of Geology, v. 77, p. 505–543.

Denlinger, R.P., and O'Connell, D.R.H., 2010, Simulations of cataclysmic outburst floods from Pleistocene glacial Lake Missoula: Geological Society of America Bulletin, v. 122, no. 5–6, p. 678–689, https://doi.org/10.1130/B26454.1.

Denlinger, R.P., O'Connell, D.R.H., and House, P.K., 2001, Robust determination of stage and discharge: An example from an extreme flood on the Verde River, Arizona, *in* House, P.K., Webb, R.H., Baker, V.R., and Levish, D.R., eds., Ancient Floods, Modern Hazards: Principles and Applications of Paleoflood Hydrology, Volume 5: Washington D.C., American Geophysical Union, p. 127–146.

George, D.L., 2008, Augmented Riemann solvers for the depth-averaged equations over variable topography with steady states and inundation: Journal of Computational Physics, v. 227, no. 6, p. 3089–3113, https://doi.org/10.1016/j.jcp.2007.10.027.

George, D.L., 2011, Adaptive finite volume methods with well-balanced Riemann solvers for modeling floods in rugged terrain: Application to the Malpasset dam-break flood (France 1959): International Journal for Numerical Methods in Fluids, v. 66, no. 8, p. 1000–1018, https://doi.org/10.1002/fld.2298.

Hanson, L.G., 1970, The Origin and Deformation of Moses Coulee and Other Scabland Features on the Waterville Plateau, Washington [Ph.D. thesis]: Seattle, University of Washington, 137 p.

Hanson, M.A., Lian, O.B., and Clague, J.J., 2012, The sequence and timing of large late Pleistocene floods from glacial Lake Missoula: Quaternary Science Reviews, v. 31, p. 67–81, https://doi.org/10.1016/j.quascirev.2011.11.009.

Higgins, J.D., Fragaszy, R.J., and Beard, L.D., 1985, Development of Guidelines for Cuts in Loess Soils: Washington Department of Transportation Report WARD-69.1, 105 p.

LeVeque, R., 2002, Finite Volume Methods for Hyperbolic Problems: Cambridge, UK, Cambridge University Press, 558 p., https://doi.org/10.1017/CBO9780511791253.

Normark, W.R., and Reid, J.A., 2003, Extensive deposits on the Pacific plate from late Pleistocene North America glacial lake outbursts: The Journal of Geology, v. 111, no. 6, p. 617–637, doi:10.1086/378334.

O'Connor, J.E., and Baker, V.R., 1992, Magnitudes and implications of peak discharges from glacial Lake Missoula: Geological Society of America Bulletin, v. 104, p. 267–279, https://doi.org/10.1130/0016-7606(1992)104<0267:MAIOPD>2.3.CO;2.

Villanueva, I., Herget, J., Wright, N., Borodavko, P., and Morvan, H., 2010, Unsteady 1D and 2D hydraulic models with ice dam break for Quaternary megaflood, Altai Mountains, southern Siberia: Global and Planetary Change, v. 70, p. 24–34, https://doi.org/10.1016/j.gloplacha.2009.11.005.

Waitt, R.B., 1980, About forty last-glacial Lake Missoula jökulhlaups through southern Washington: The Journal of Geology, v. 88, p. 653–679, https://doi.org/10.1086/628553.

Waitt, R.B., 1984, Periodic jökulhlaups from Pleistocene glacial Lake Missoula—New evidence from varved sediment in northern Idaho and Washington: Quaternary Research, v. 22, p. 46–58, https://doi.org/10.1016/0033-5894(84)90005-X.

Waitt, R.B., 1985, Case for periodic, colossal jökulhlaups from Pleistocene glacial Lake Missoula: Geological Society of America Bulletin, v. 96, p. 1271–1286, https://doi.org/10.1130/0016-7606(1985)96<1271:CFPCJF>2.0.CO;2.

Waitt, R.B., 1994, Scores of gigantic, successively smaller Lake Missoula floods through the Channeled Scabland and Columbia River valley, *in* Swanson, D.A., and Haugerud, R.A., eds., Geologic Field Trips in the Pacific Northwest, Volume 1: Seattle, Washington, Department of Geological Sciences, University of Washington, p. 88.

Waitt, R.B., 2016, Megafloods and Clovis Cache at Wenatchee, Washington: Quaternary Research, v. 85, p. 430–444, https://doi.org/10.1016/j.yqres.2016.02.007.

Waitt, R.B., 2021, this volume, Roads less travelled by—Pleistocene piracy in Washington's northwestern Channeled Scabland, *in* Waitt, R.B., Thackray, G.D., and Gillespie, A.R., eds., Untangling the Quaternary Period—A Legacy of Stephen C. Porter: Geological Society of America Special Paper 548, https://doi.org/10.1130/2021.2548(18).

Waitt, R.B., and Thorson, R.M., 1983, The Cordilleran ice sheet in Washington, Idaho, and Montana, *in* Porter, S.C., ed., Late Pleistocene Environments: Late Quaternary Environments of the United States: Minneapolis, Minnesota, University of Minnesota Press, p. 58–70.

Waitt, R.B., Denlinger, R.P., and O'Connor, J.E., 2009, Many monstrous Missoula floods down Channeled Scabland and Columbia Valley, *in* O'Connor, J.E., Dorsey, R.J., and Madin, I.P., eds., Volcanoes to Vineyards: Geologic Field Trips through the Dynamic Landscape of the Pacific Northwest: Geological Society of America Field Guide 15, p. 775–844, https://doi.org/10.1130/2009.fld015(33).

Waitt, R.B., Breckenridge, R.M., Kiver, E.P., and Stradling, D.F., 2016, Late Wisconsin Cordilleran ice sheet and colossal floods in northeast Washington and north Idaho, *in* Cheney, E.S., ed., The Geology of Washington and Beyond—From Laurentia to Cascadia: Seattle, Washington, University of Washington Press, p. 233–256.

Waitt, R.B., Long, W.A., and Stanton, K., 2019, Erratics and other evidence of late Wisconsin Missoula outburst floods in lower Wenatchee and Columbia River valleys, Washington: Northwest Science, v. 92, no. 5, p. 318–337.

Manuscript Accepted by the Society 28 May 2020

Printed in the USA